A Simple Diagnosis Tool for Detecting Localized Roughness Features

Karim Chatti, Associate Professor[1]
Imen Zaabar, Graduate Research Assistant[2]
Hyung Suk Lee, Staff Engineer[3]

Abstract

The collection of distress data from video imaging of the pavement surface can provide the location and type of many distresses. However, it cannot provide useful information about some distress features such as the magnitude of faulting, breaks and curling in concrete pavements. This paper describes a simple tool to extract such information through the use of the raw profile data. Different methods were used in the study, including wavelets, time-frequency and discrete methods. The discrete elevation difference method (DED) was selected for faulting and breaks detection, and the discrete slope method (DS) was selected for curling detection. To test the validity of the analysis, surveys were conducted on different sites in Michigan. Faults magnitude was measured using Georgia faultmeter and the location of the distress is measured using measuring wheel. The profile data for the same pavement section where collected using the a high speed profilometer. The new tool was able to detect the magnitude of faulting and breaks with an average error of 0.1% and a standard deviation of 1%. The localization was also highly accurate (average error in distance is within 1 m or 0.5%). The results indicate that the methods described above can capture relevant information about these roughness features with reasonable accuracy.

Keywords: Detection, Roughness features, Discrete elevation difference, Discrete slope method.

Introduction

Road roughness indices such as the International Roughness Index (IRI) and Ride Quality Index (RQI) are useful as indicators of the level of pavement serviceability. Each of these summary roughness statistics offers a convenient index for monitoring the trend of pavement roughness deterioration with time. However, they do not retain the actual contents of pavement surface roughness. Such detailed roughness information may be useful for maintenance operations, and detection of roughness features. The collection of distress data from video images of the pavement surface can provide the location and type of many distresses. However, because video images of pavement surface are two-dimensional, they cannot quantify pavement surface characteristics. Therefore, such

[1] Department of Civil and Environmental Engineering, Michigan State University, 3546 Engineering Building, East Lansing, MI-48824, USA, Email: chatti@egr.msu.edu
[2] Department of Civil and Environmental Engineering, Michigan State University, MI, USA. zaabarim@msu.edu
[3] State Materials Office, Materials Research Park, Applied Research Associates, Inc 5007 NE 39th Avenue, Gainesville, FL 32609-2604,USA. hlee@ara.com

images cannot provide useful information about roughness features, including their magnitude and location. Failure to include specific roughness features in Pavement Management Systems (PMS) has the following negative impacts on system performance:

- The analysis may overestimate the Remaining Service Life (RSL) of the pavement.
- The system process may not ultimately select the most cost-effective fix to extend pavement life.
- Missing information on specific roughness features reduces the reliability of recommending the most cost-effective strategy for preserving the pavement network.

This paper describes simple tools to extract such information through the use of the raw profile data. This new tool can provide a better representation of certain roughness features.

Background

Michigan Department Of Transportation's (MDOT) Pavement Management System extracts pavement surface distresses (type, extend, and severity) from video images of the pavement surface bi-annually. The raw profile is collected by a high speed profilometer. Surface distresses and profile data of all pavement types (rigid, flexible, and composite) are used to automatically compute Distress Index (DI) and Ride Quality Index (RQI), for a minimum segment length of 161 m (0.1 mile). The bi-annual change of the pavement's DI is included in a performance model to estimate the pavement's RSL. RQI reflects the user's perception about pavement ride quality, whereas, surface distresses are related to possible structural failures of the pavement. The RQI and DI describe the condition of a pavement section at a given point in time, while RSL is a performance estimation of a pavement section.

Distresses. Distress is an important factor in pavement design and management. The evaluation of pavement distress is an important part of the pavement management system by which a most effective strategy for maintenance and rehabilitation can be developed. Our concern in this paper is the detection of faults, breaks and curling in concrete pavements.

Filtering out the road geometry curve: Butterworth Filters. A number of approaches have been used for removing the long-wave topography from the measured profile. The principles of several filtering techniques have been discussed in the pavement smoothness literature (Shokouhi et al., 2006). The Butterworth filters are the most appropriate for our application since they have the following characteristics (Orfanidis, 1996):

- Smooth response at all frequencies
- Monotonic decrease from the specified cut-off frequencies
- Maximal flatness, with the ideal response of unity in the passband and zero otherwise.
- Half-power frequency, or 3 dB down frequency, that corresponds to the specified cut-off frequencies

Figure 1 (a) shows the frequency response of a low-pass Butterworth filter. However, these filters always create phase distortion. Butterworth filters can be modified to become zero-lag filters when the data are processed in both the forward and reverse directions. In such cases little improvement is realized by applying multiple passes. The overall filter is implemented by cascading all passes in series. This solution was first introduced by Murphy and Robertson (1994). Therefore, the Butterworth filters may still be the best choice.

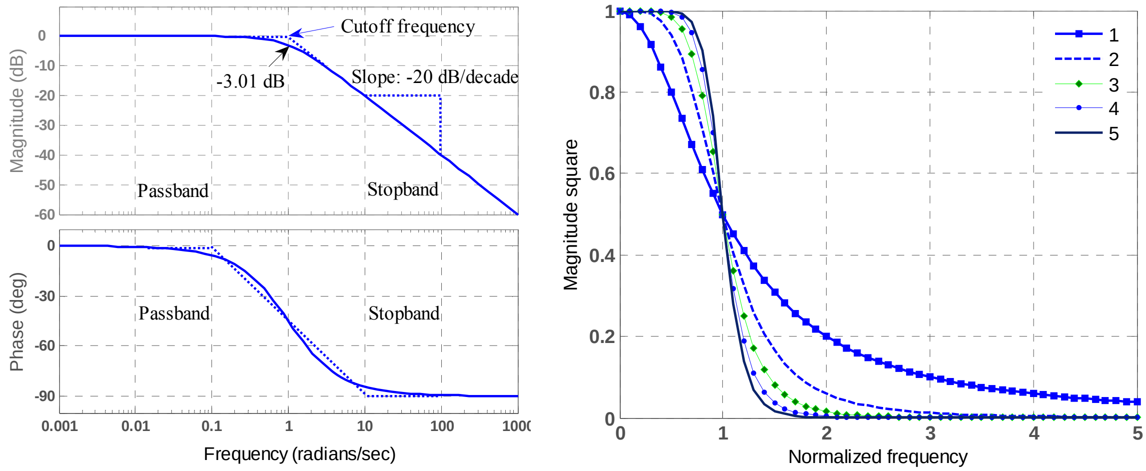

(a) (b)

Figure 1 – (a) Butterworth filter bode plot (b) Transfer functions of the Butterworth filter for various orders

Methods to identify roughness features. Although considerable information on profile analysis is documented, only few studies that discuss diagnosing/localizing distresses from the actual profile data identify the type of distresses.

De Pont et al. (1999) introduced wavelets to be used for identifying the local features of the profile. The suggested method localizes features of the profile in terms of short, medium and long wavelengths. However, the method does not identify the individual distresses that are present. De Pont also discussed the usefulness of the wavelets in terms of compressing the profile data for storage. From his example, the profile data were compressed into only 5% of the size of the original signal, and the reconstructed signal had a maximum difference of 3 mm (0.12 in) in comparison to the original signal. Figure 2(a) shows example outputs from Matlab® using the above procedure to detect distresses with discrete wavelet transforms.

Figure 2(b) shows similar outputs using continuous wavelet transforms. The highlighted locations in Figure 2(a) may potentially represent faulting or cracking since they show high variations in the decomposed signal. The wavelets used were Daubechies (db) wavelets, which are widely used in engineering applications because there are the only orthogonal wavelets (allowing unique reconstruction of the original signal) that can be used in both continuous and discrete analysis.

Byrum (2001) developed an algorithm that picks up the "imperfection" zone from the profile of rigid pavements. These zones are then separated from the slab region.

However, the method does not identify the type of the individual distresses that are present. The detection of the imperfection zone is done by calculating the curvature of the

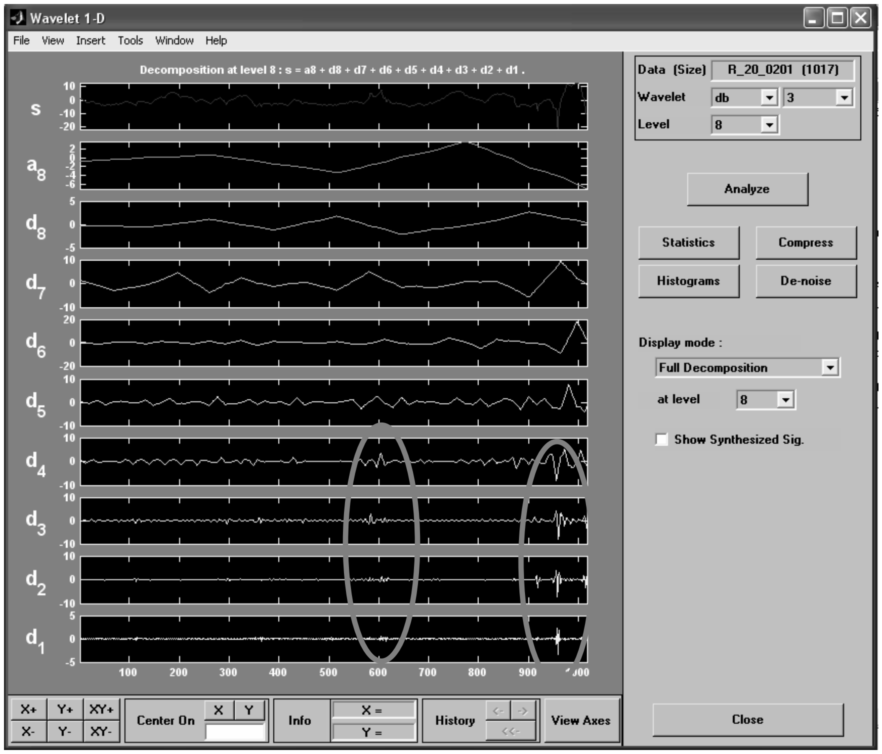

(a)

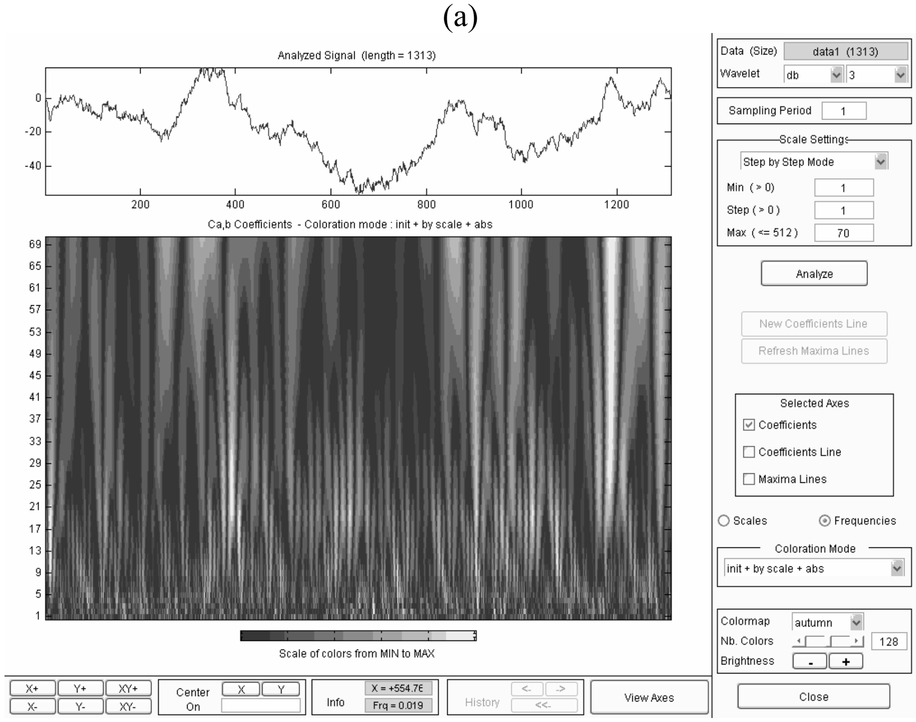

(b)

Figure 2 – Example outputs from distress detection procedure using (a) continuous and (b)discrete wavelet transform

profile and applying a threshold on the curvature. The threshold value for CVT is between 10 mm^{-1} and 49 mm^{-1}. The curvature variation threshold (CVT) is calculated by the following equation:

$$CVT = \frac{1}{12}\left[-0.03242(06CVStDev)^{0.8405} + 0.00665(24CVStDev)^{1.1446} - 0.06631(48CVStDev)^{3.7819}\right]$$

(0.003 < CVT < 0.015 ft^{-1}; 1 ft = 0.3048 m); $R^2 = 0.81$

where 06CVStDev = Standard deviation of the 152.4-mm curvatures in 152.4 m profile, 1/ft *1000
24CVStDev = Standard deviation of the 609.6-mm curvatures in 152.4 m profile, 1/ft *1000
48CVStDev = Standard deviation of the 1219.2-mm curvatures in 152.4 m profile, 1/ft *1000

Fernando and Bertrand (2002) used moving average filters to detect localized roughness. The points where the deviations from the averaged profile are large are the rough areas. However, this method does not identify the actual distresses.

Chang et al. (ProVAL Software, Transtec Group) identified localized roughness based on the Texas Department of Transportation Specification Tex-1001-S. This method was first used by Fernando et al. (2002). First, each elevation point from the two longitudinal profiles (left and right wheel paths) is averaged to produce a single averaged wheel path profile. Then, the resulted profile is placed on a 7.6 m (25 ft), centered-moving average filter. The difference between the average wheel path profile and the 7.6m-moving average filtered profile for every profile point is computed. Deviations greater than 3.8 mm (0.15 in) are considered a detected area of localized roughness. Positive deviations are considered as "bumps" and negative ones as "dips". However, this method does not identify the distress type.

Localized Roughness Detection Methods

Five methods were considered in this study for identifying roughness features from a profile: (1) Discrete Elevation Difference method (DED); (2) Discrete Slope method (DS); (3) Discrete Curvature method (DC); (4) Wavelet analysis method; and (5) Time-frequency analysis. Many time-frequency analysis approaches were performed during this analysis including Wigner-Ville Distribution (WVD), Pseudo WVD (PWVD), and Smoothed Pseudo WVD (SPWVD), Short Time Fourier Transform (STFT) using different cutoff windows (Hamming, Hanning, Gabor distribution, etc). Although, the joint time frequency analysis method is powerful for electrical and mechanical signals, it was found not to be effective for the analysis of pavement profiles. Specifically, the following issues were noted:

1. The non-linearity of the Wigner distribution causes many interference phenomena, which make it less attractive for detection purposes.
2. A different approach to obtain a local time-frequency analysis (suggested by various scientists, among them Ville), is to cut the signal first into slices, followed by doing a Fourier analysis on these slices. However, the functions obtained by this crude segmentation are not periodic, which will be reflected in large Fourier coefficients at high frequencies, since the Fourier transform will interpret this jump at the boundaries as a discontinuity or an abrupt variation of the signal.
3. The STFT has also its disadvantages, such as the limit in its time-frequency resolution capability, which is due to the uncertainty principle. Low frequencies can be hardly depicted with short windows, whereas short pulses can only be

poorly localized in time with long windows. These limitations in the resolution were some of the reasons for the invention of Wavelet theory.

It was found that the wavelet analysis, the DED and DS methods give better results. These methods were able to extract the magnitude and location of distresses with the same order of error. However, the DED and DS method were selected in this study for their simplicity. The DED method was selected for detecting faults and breaks. The DS method was selected for curling detection. An example comparing observed versus predicted faults from DED and wavelet methods using a real profile is shown in figure 3.

Fault Detection. The discrete elevation difference method consists of computing the difference in elevation between points at a given interval. Theoretically, when the samples of the profile are collected over a faulted joint/crack, the difference in elevation should appear in two adjacent samples. However, the faulting of the slab in the raw profile (collected by MDOT) appears at several sample points (Figure 4). As seen in figure 5, the elevation is collected at every 19 mm (0.75 in) [sampling interval] and recorded at every 76.2 mm (3 in) [recording interval]. Consequently, when the difference in elevation is computed, each fault/crack is represented by a range of differences. Thus, the largest absolute value (local maximum) for each range of differences was taken as the fault magnitude. However, as it can be seen from figure 6, if the faulting is calculated based on the elevation difference of adjacent points, three different values of the fault magnitude can be obtained, depending on whether the distance to the fault is a multiple of the recording interval:

- Exact magnitude: Figure 6 (a),
- 75% of the exact magnitude: Figure 6 (b) and (d)
- 50% of the exact magnitude: Figure 6 (c)

In order to resolve this problem, it was decided to take the difference in elevation between the points that are 152 mm (6 in) apart (±76 mm of the point of interest).

Figure 8 presents the fault detection algorithm. The threshold value T is left as an input to the algorithm. It is based on the user judgment. For the analyses presented herein, a T –value of 1mm was used.

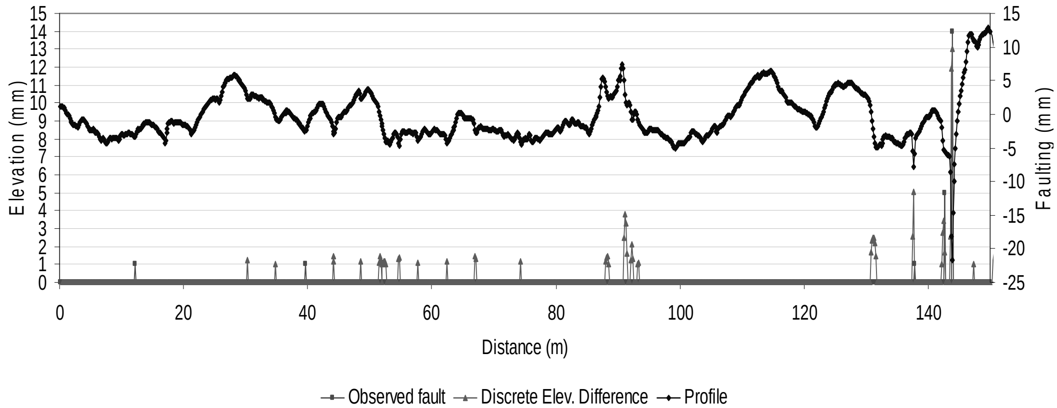

(a) Discrete elevation difference method

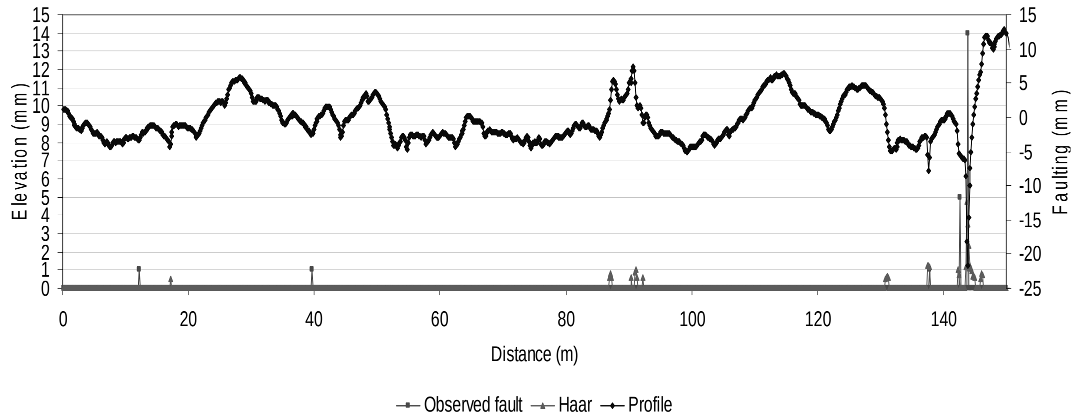

(b) Wavelet (Haar) method

Figure 3 – Comparison of fault detection from (a) discrete elevation and (b) wavelet methods

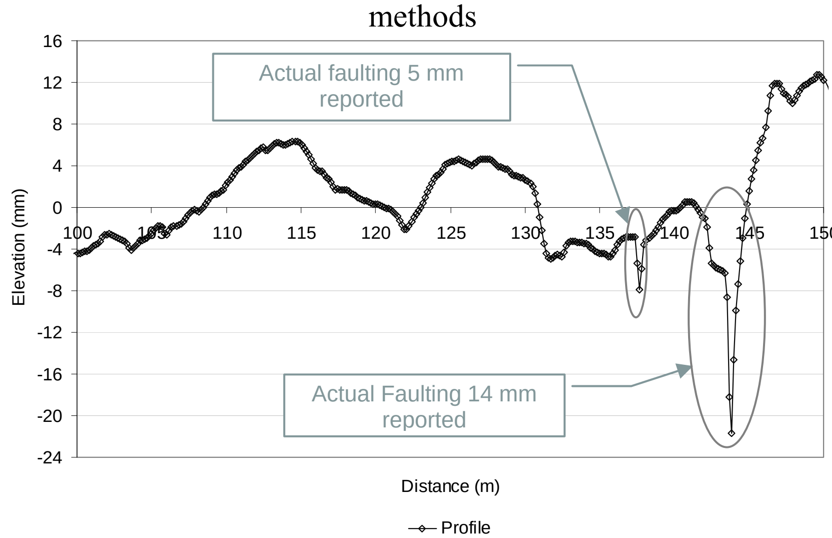

Figure 4 – Faulting in the raw profile

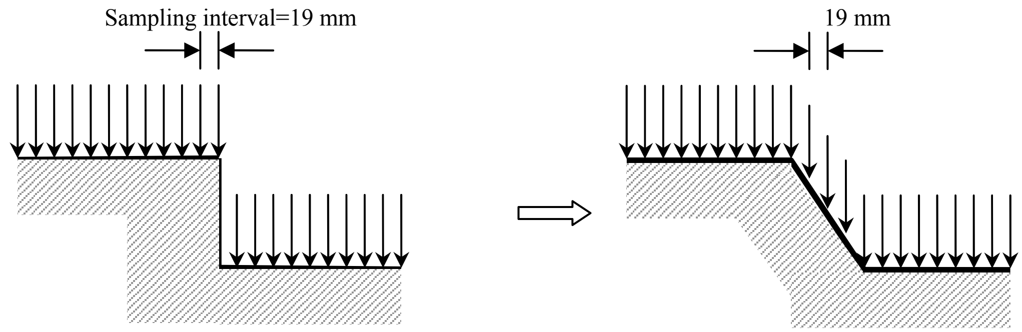

Figure 5 – Effect of the moving average filter on surface discontinuity

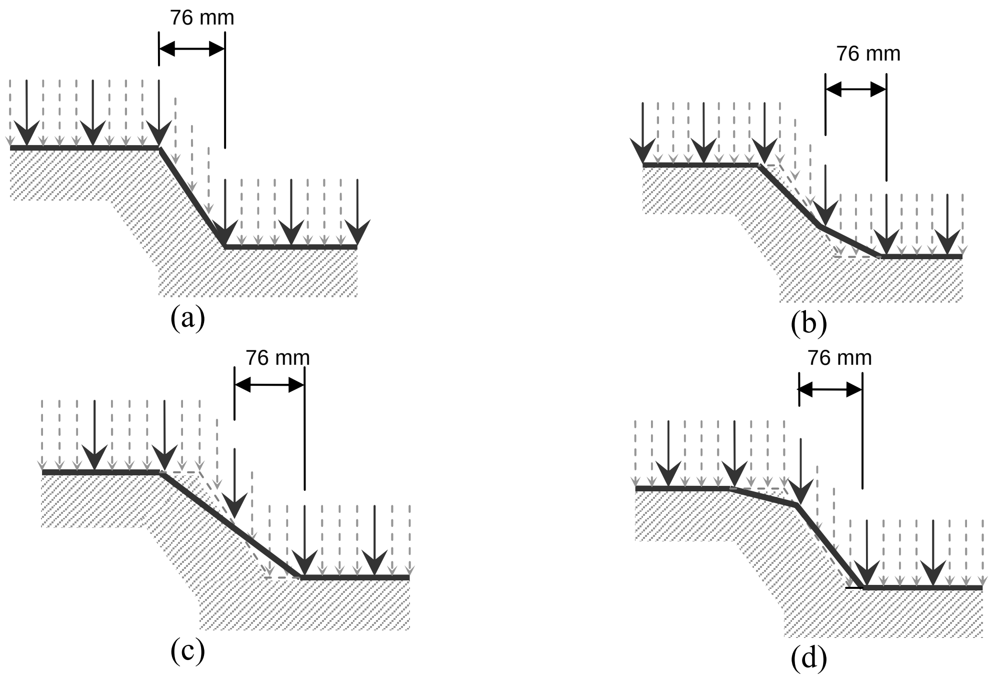

Figure 6 – Different scenarios of recording a fault after filtering

Breaks Detection. For the detection of breaks, 0.9 m (3 ft) was considered as a maximum threshold for the width (Figure 7). Before detecting breaks, different steps are followed. First, differences in elevation are computed. This step is the same as the fault detection method. Second, if the sign of two successive faults is different, the method checks the distance between them: if the distance is less than 0.9 m, it is considered break; otherwise, there is no break. Figure 8 shows the break detection algorithm.

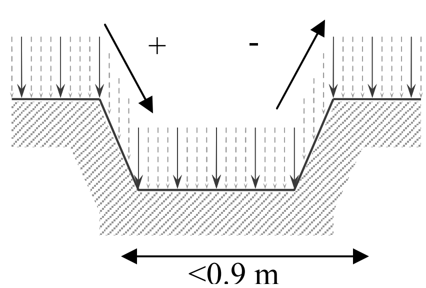

Figure 7- Schematic of a break

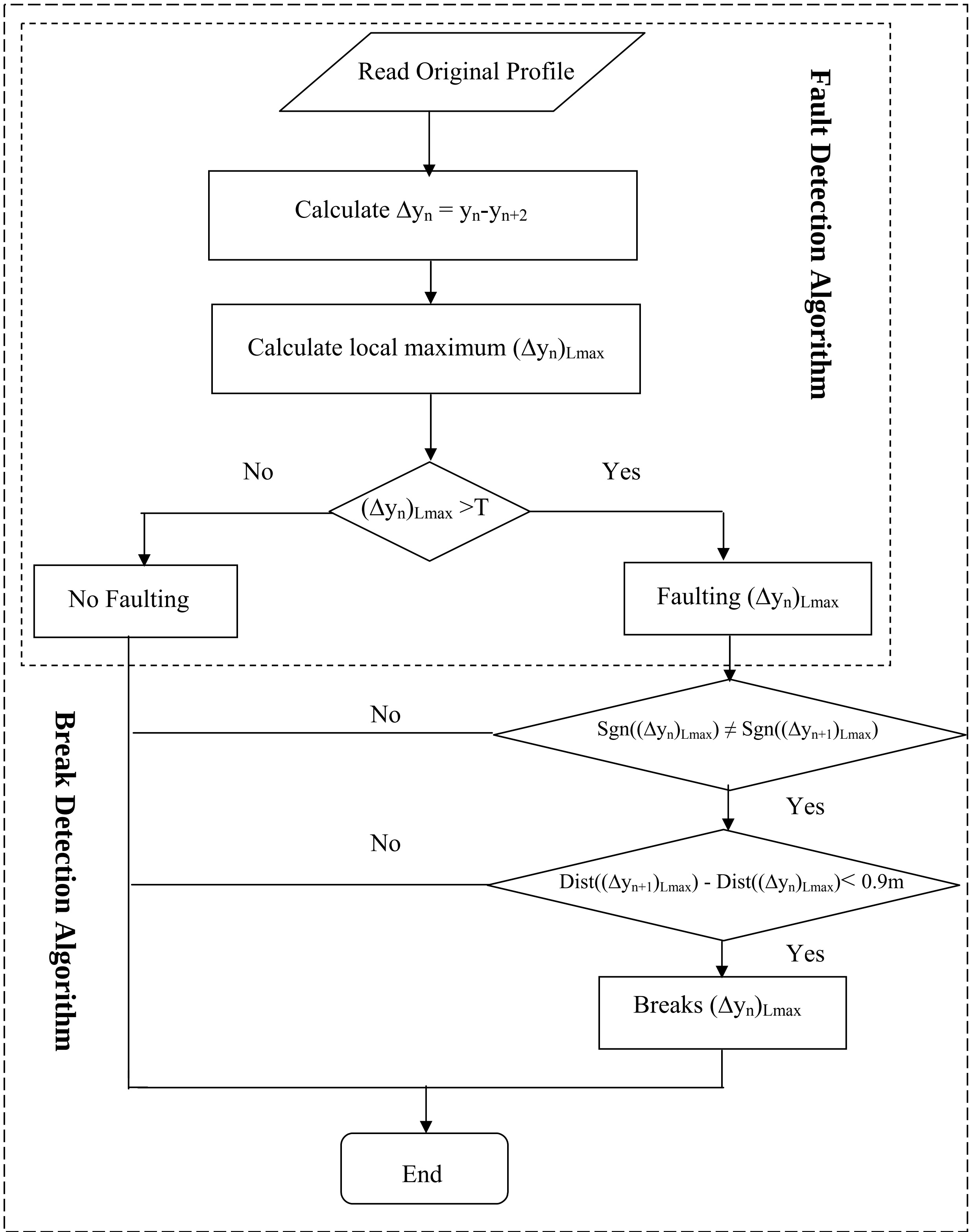

Figure 8- Fault and Break detection algorithm

Curling Detection. Since we are looking for discontinuities in the slope of the profile, the discrete slope (DS) method was selected to detect slab curling. This method has been used in signal and image processing for its capability to detect discontinuities. It is similar to the DED method in the sense that it takes the difference in elevation. But the difference is that the slope (difference in elevation divided by the distance between the points) is taken from the adjacent sample points. Figure 9 shows a simulated profile and the corresponding slope. It is noted that the topography has an impact on the roughness features detection. To filter out the topography, a high-pass filter (91.45 m or 300 ft long cut-off wavelength) was applied. Then, to eliminate the effect of profile roughness and micro-curling, a low-pass filter (1.52 m or 5 ft short cut-off wavelength) was applied. Figure 10 shows the results after each step.

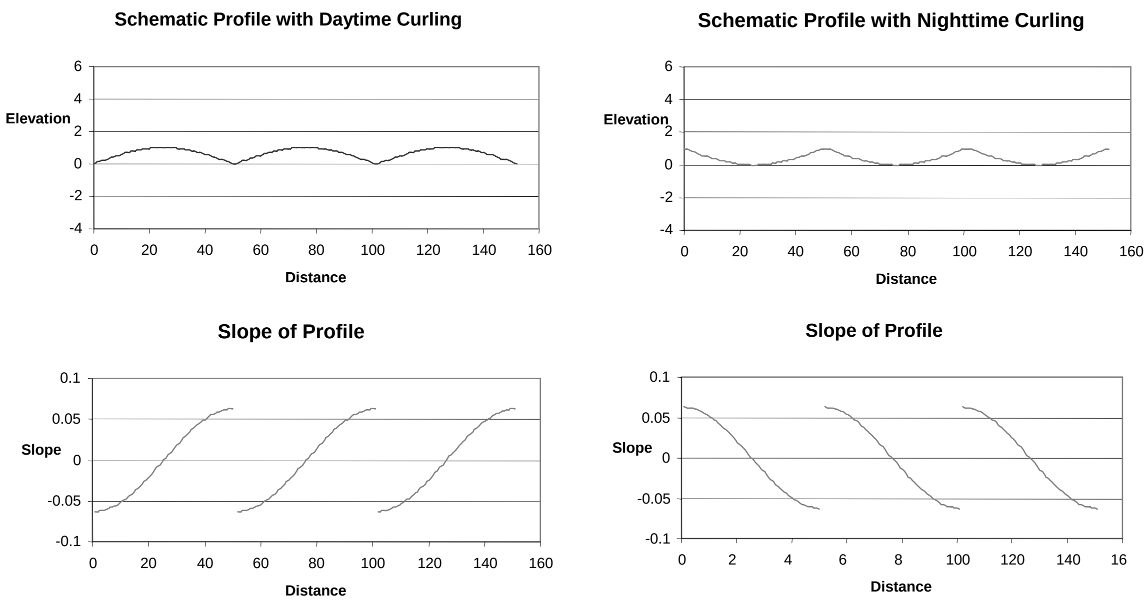

Figure 9- Extraction of curling features from simulated profiles using discrete slope method

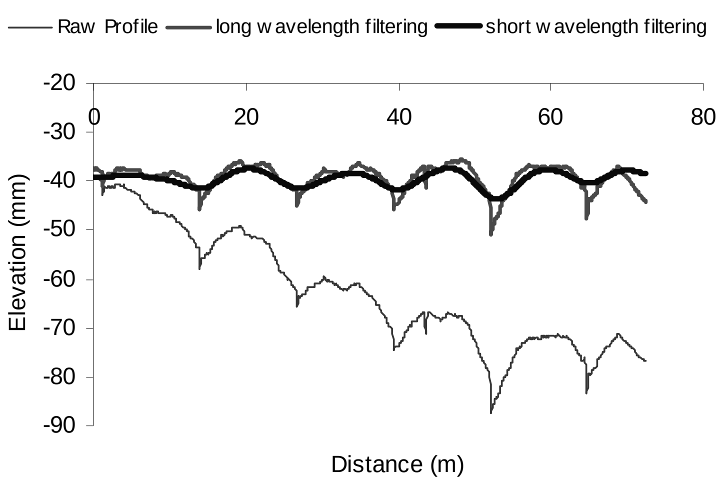

Figure 10- Original and filtered profiles

Different types of filters (e.g. moving average, 2-pole Butterworth, 4-pole Butterworth (Sayers et al., 1996), etc.) were used. Since a 2-pole Butterworth filter add a phase lag to the filtered profile, a 4-pole Butterworth was needed.

Finally, to compute curling, differences in elevation between the point that corresponds to the local maximum of the slope function and the next point where the slope function is zero is computed (Figure 11). Figure 12 shows the curling detection algorithm.

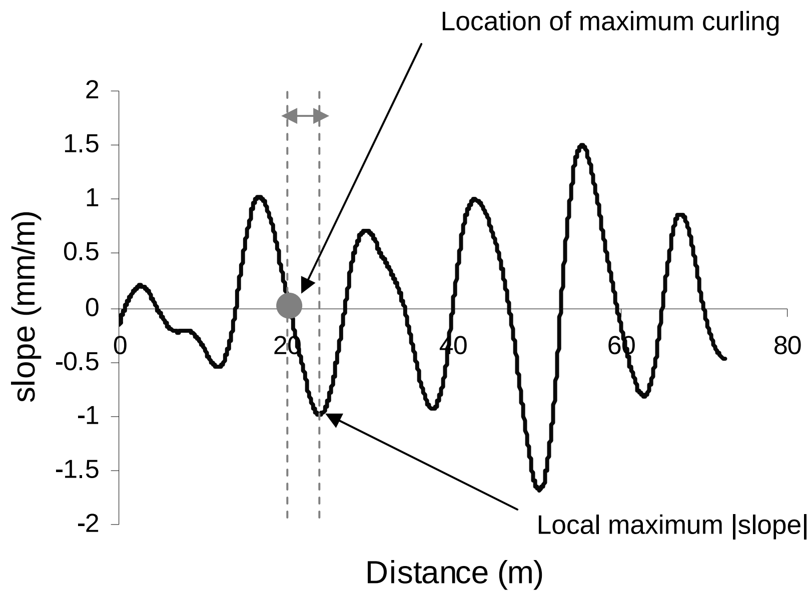

Figure 11- Detection of local maxima of the slope function

Results and validation

Field tests were conducted at three sites in Michigan. The concrete pavements for all sites had a joint spacing of 12.5 m (41 ft). Site 1 and site 2 were approximately 856 m (0.52 miles) long and experienced many faulted cracks. Site 3 was approximately 1384 m (0.86 miles) long. In each site, faults/breaks were measured using a digital faultmeter (also called the Georgia faultmeter) at the left and right wheel paths (Figure 13). Repeated measurements were taken to evaluate the accuracy of the measurement device. The error was found to be equal to 0.2%. The location of the distress was measured using the distance measuring wheel. Table 1 defines the severity level, and Table 2 summarizes the number of measured faults in terms of the severity level and the minimum/maximum values of fault magnitude in each site. In order to independently verify the methods using the manually collected data, the profile data for the same pavement sections collected using the high speed profilometer were requested to be used in the developed algorithms.

Statistical analyses were performed to study the accuracy of the method. Figures 14, 15 and 16 show the results obtained from these analyses. As can be seen from these figures, the predicted magnitude and location of faults for each site match well with the measured magnitude and location. However, each figure show a bias, all be it very small; this error could be the result of inattention in fault measurements or inaccuracy of profile data. Comparing the slopes from successive figures, it can be seen that the bias in the measurements was slightly reduced after each field test (slope value closer to unity).

Therefore, we conclude that the DED method is able to detect the location of a fault and compute its magnitude with a reasonable accuracy.

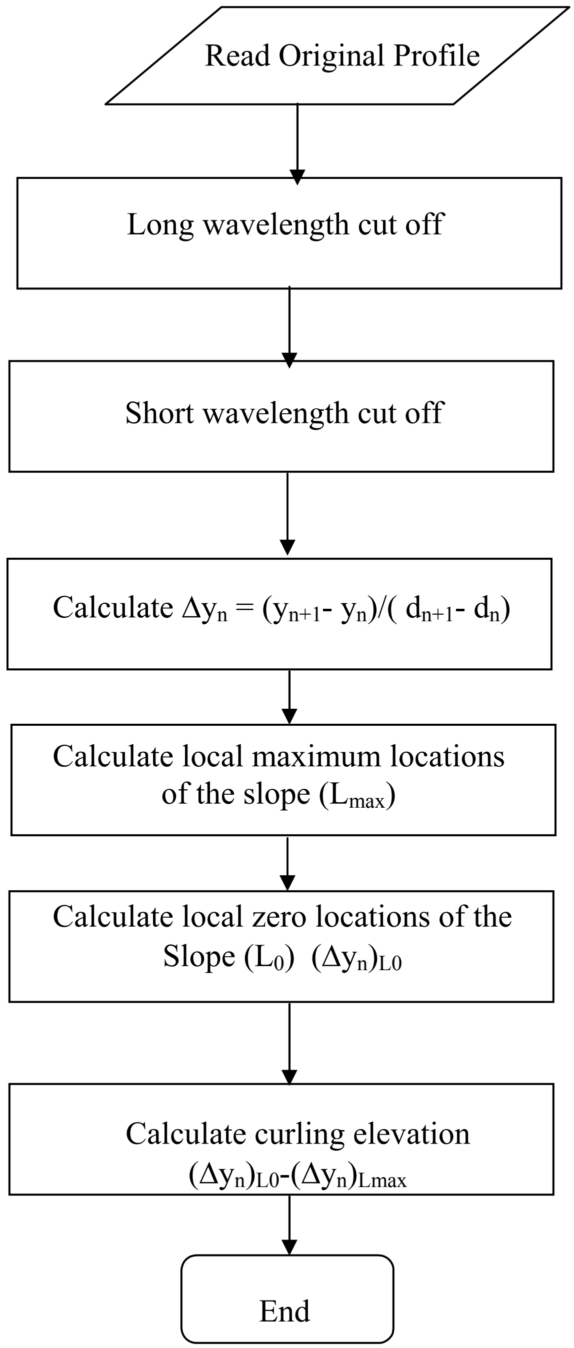

Figure 12 Curling detection algorithm

Figure 13- Field trials equipement and set up

Table 1- Definition of severity level

	Severity Level		
Distress Type	Low (L)	Medium (M)	High (H)
Faults, Breaks, Bumps and Depression	≤ 6.35 mm	≥ 6.35 mm, ≤ 19 mm	≥ 19 mm

Table 2- Summary of measured faults from field trials in each section

	Site 1				Site 2				Site 3			
Severity level	L	M	H	Total	L	M	H	Total	L	M	H	Total
Number	124	4	0	128	57	12	0	69	150	48	0	198
Max. value (mm)	14.22				9.65				13.72			
Min. value (mm)	-3				-3.8				-10.9			

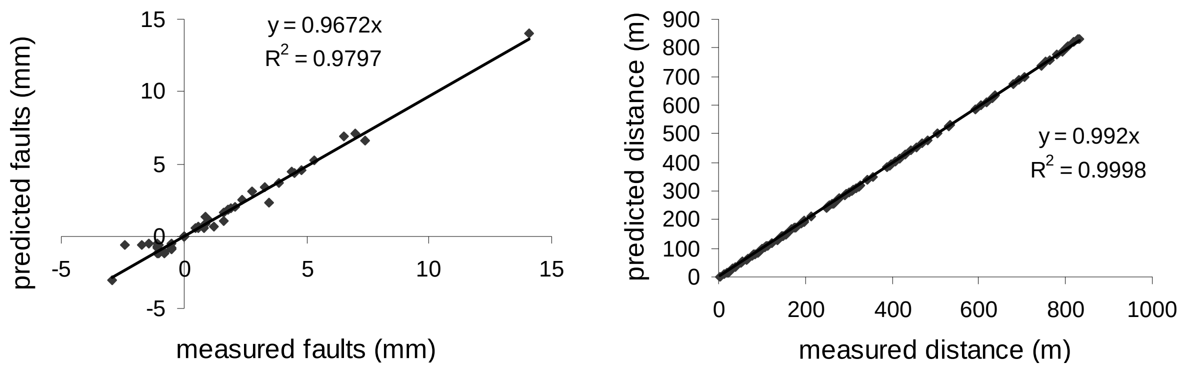

(a) (b)

Figure 14- Correlation analyses for Site 1 (a) magnitude (b) location

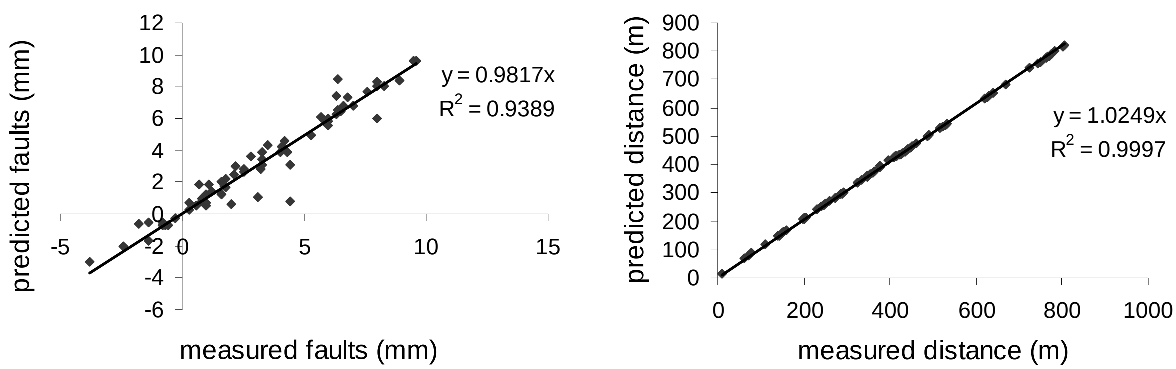

(a) (b)

Figure 15- Correlation analyses for Site 2 (a) magnitude (b) location

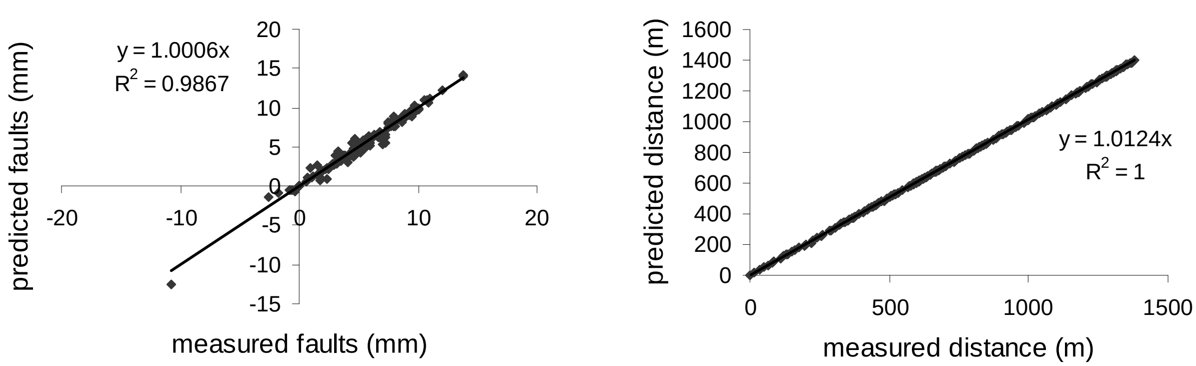

(a) (b)

Figure 16- Correlation analyses for Site 3 (a) magnitude (b) location

Three breaks were reported during the field test in Site 1. The tool was also able to detect all three breaks with a comparable magnitude and location. Table 3 summarizes the number of observed and predicted breaks, their width and magnitude for all the sites.

Table 3- Summary of observed breaks from field trials and predicted breaks using the algorithm

	Starting point (m)		Width (m)		Fault magnitude at the starting point (mm)		Fault magnitude at the end (mm)	
Break number	Observed	Predicted	Observed	Predicted	Observed	Predicted	Observed	Predicted
1	220.1	221.2	0.14	0.15	3	3.05	-4.3	-4.35
2	321	321.7	0.14	0.15	3	3.05	-5.4	-5.38
3	623.7	624.3	0.5	0.53	12	12.06	-14.22	-14.18

Site 1 also had severe daytime curling (Figure 17). The tool was also able to detect the curling magnitude and frequency (Figure 18).

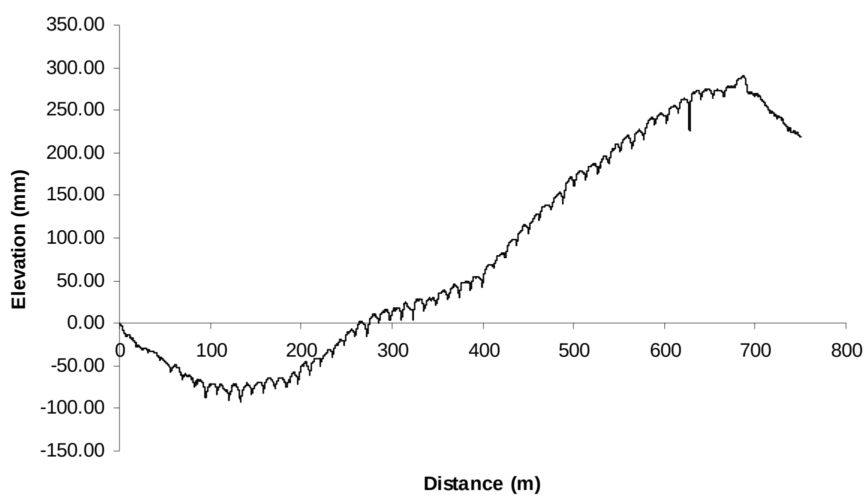

Figure 17- The raw profile for Site 1

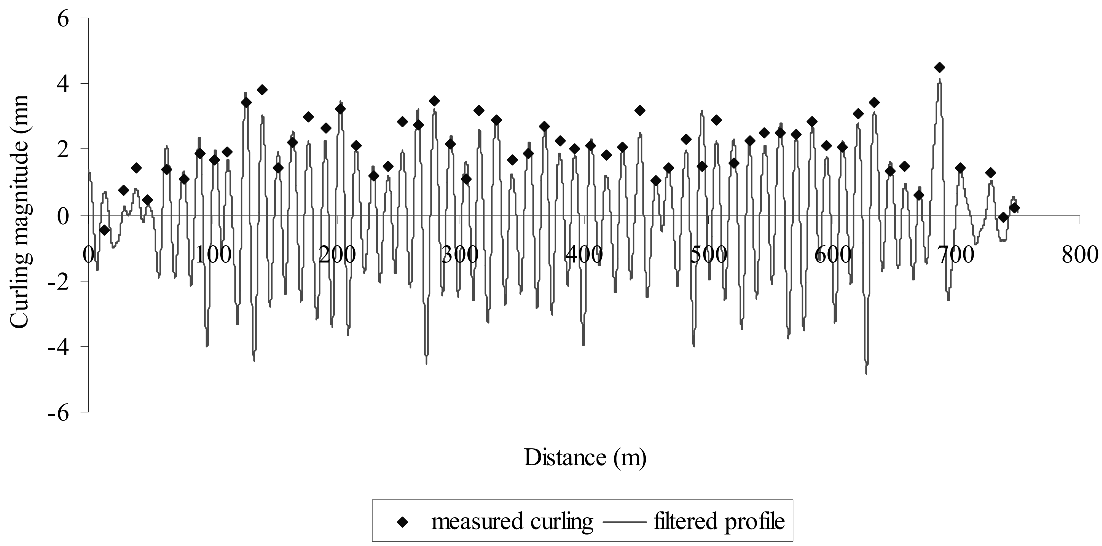

Figure 18- Filtered profile and predicted curling magnitude

Conclusion

In this paper, we showed that the new developed tool was able to detect, identify, and localize roughness features that are not readily available from video imaging methods. We proved that the methods discussed above give results with a comparable magnitude and frequency of faulting and breaks with an average error of 0.1% and a standard deviation of 1%. The localization was also highly accurate (average error in distance is within 1 m or 0.5%). Thus, this new tool could be used as a complementing module for the existing PMS. It would help the highway agencies in deciding whether a particular section of the pavement needs a maintenance/rehabilitation action.

References

Byrum, C. (2001) "A high speed profiler based slab curvature index for jointed concrete pavement curling and warping analysis". Ph.D Dissertation. University of Michigan.

De Pont and Scott, J.J. (1999), "*Beyond road roughness-interpreting road profile data*", Road & Transport Research, v8, 12-28.

Fernando, E. and Bertrand, C. (2002), "*Application of profile data to detect localized roughness*", Transportation Research Record, 1813, 02-4050, 55-61.

Murphy, S.D. and Robertson D.G.E. (1994), "*Construction of a high-pass digital filter from a low-pass digital filter*", Journal of Applied Biomechanics, 10 (1994) 374–381

Orfanidis, S.J. (1996), *Introduction to signal Processing*, Prentice-Hall, Upper Saddle River, New Jersey.

ProVAL 2.7, a software for pavement profile viewing and analysis, The Transtec Group, available for download at www.roadprofile.com.

Sayers and Karamihas (1997), *Interpretation of Road Roughness*, UMTRI 96-19.

Shokouhi, P., Gucunski, N., Maher, A., Zaghloul, S. M. and Vitillo, N. P., "*Advanced Analysis of Pavement Profiles*". Proceedings of the 85th TRB annual Meeting, TRB, 2006, Washington, D.C.